KURENAI
Kyoto University Research Information Repository

KYOTO UNIVERSITY

Title	Hexagonal rare earth-iron mixed oxides (REFeO): Crystal structure, synthesis, and catalytic properties
Author(s)	Hosokawa, Saburo
Citation	Frontiers in Chemistry (2019), 7
Issue Date	2019-01-28
URL	http://hdl.handle.net/2433/236479
Right	© 2019 Hosokawa. This is an open-access article distributed under the terms of the Creative Commons Attribution License (CC BY). The use, distribution or reproduction in other forums is permitted, provided the original author(s) and the copyright owner(s) are credited and that the original publication in this journal is cited, in accordance with accepted academic practice. No use, distribution or reproduction is permitted which does not comply with these terms.
Type	Journal Article
Textversion	publisher

Kyoto University

Hexagonal Rare Earth-Iron Mixed Oxides (REFeO₃): Crystal Structure, Synthesis, and Catalytic Properties

Saburo Hosokawa [1,2]*

[1] Elements Strategy Initiative for Catalysts and Batteries, Kyoto University, Kyoto, Japan, [2] Department of Molecular Engineering, Graduate School of Engineering, Kyoto University, Kyoto, Japan

The rare earth-iron mixed oxide (REFeO₃) is an attractive material in fields such as electronic, magnetic, and catalytic research. Generally, orthorhombic REFeO₃ (o-REFeO₃) with a perovskite structure is better known than hexagonal REFeO₃ (h-REFeO₃), because o-REFeO₃ is thermodynamically stable for all RE elements. However, h-REFeO₃ has a very interesting crystal structure in which a RE and Fe layer are alternately stacked along the c-axis in the unit cell; nevertheless, synthesis of the h-REFeO₃ belonging to metastable phase can be problematic. Fortunately, solution-based synthetic methods like solvothermal or coprecipitation synthesis have recently enabled the selective synthesis of h-REFeO₃ and o-REFeO₃ with comparative ease. Although the electronic and magnetic properties of h-REFeO₃ have typically been evaluated, recent research has also revealed excellent catalytic properties that enable environmental cleanup reactions such as hydrocarbon or CO oxidation. This mini-review introduces a synthetic method for controlling the crystal structure between orthorhombic and hexagonal REFeO₃ and the catalytic performance of h-REFeO₃-based materials.

Keywords: solvothermal method, coprecipitation method, catalyst, perovskite structure, hexagonal structure

INTRODUCTION

REFeO₃ (RE: rare earth) with a RE/Fe ratio of 1 are largely relevant to the perovskite structure, a structure in which RE ions are basically replaced with 1/4 of cubic close-packed oxygen ions, and Fe ions occupy all octahedral gaps formed from the remaining oxygen ions. REFeO₃ having a perovskite structure have been applied in various fields from electronic devices to catalysts. On the other hand, hexagonal REFeO₃ is known to exist as a metastable phase, but the synthetic method is very complex. Interestingly, the crystal structure has a unique coordination state for Fe³⁺ ion and is different from that of the perovskite-type REFeO₃; that is, Fe³⁺ ions in hexagonal structure have trigonal bipyramidal coordination, although Fe³⁺ ions in α-Fe₂O₃, Fe₃O₄, or perovskite-type REFeO₃ generally prefer octahedral or tetrahedral coordination. Therefore, hexagonal structure has a potential which provokes an interesting property for the above applied fields. In particular, novel catalysts composed on abundant base metal as Fe ion have been recently desired to replace the use of precious metals, such as Pt or Pd; the catalyst design based on a unique crystal structure is considered to be necessary to dramatically improve the catalytic performance of Fe-based material.
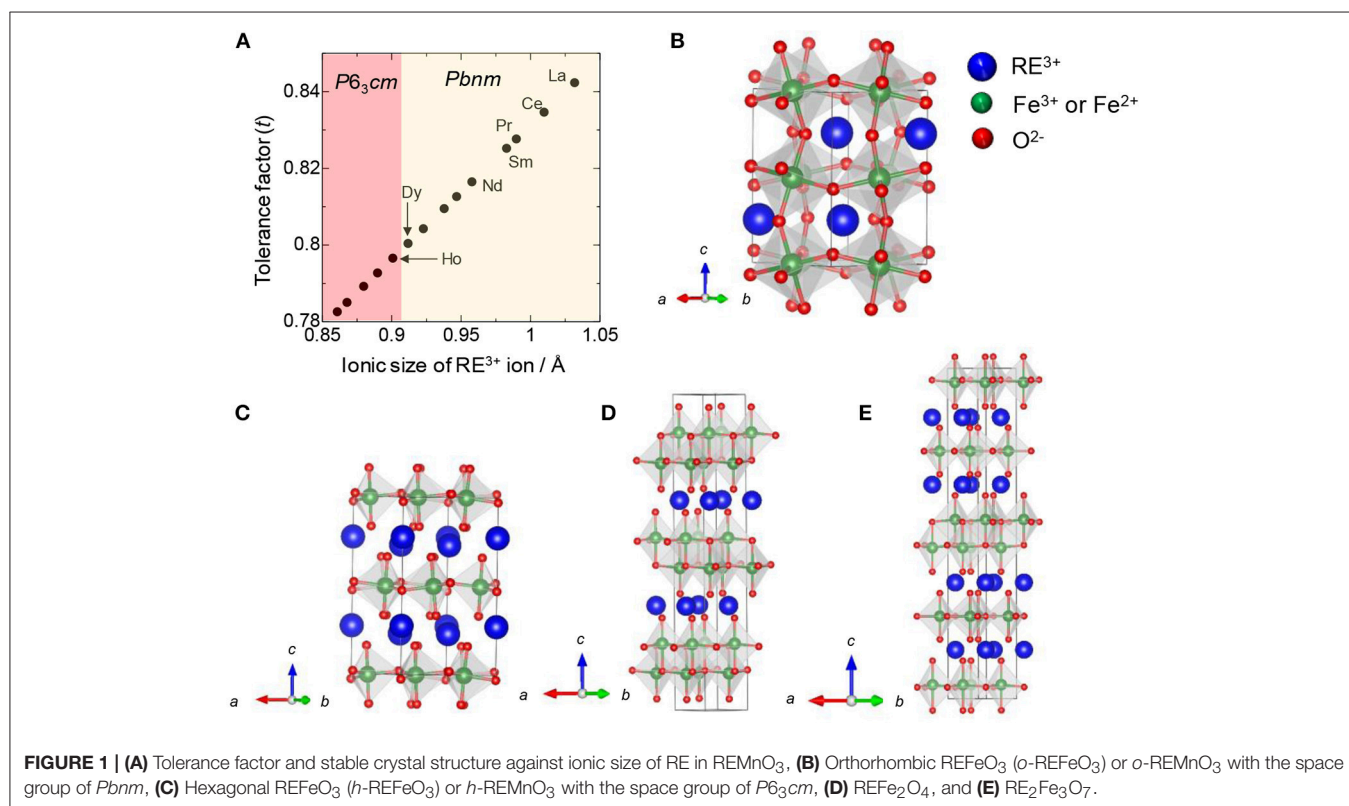
First, the relationship between RE elements and hexagonal structure is introduced, based on a general perovskite structure. Considering that each ion is in contact within the perovskite structure, the following equation is true: $(r_A + r_O) = \sqrt{2}(r_B + r_O)$, where r_A, r_B, and r_O represent the ionic radii of the A cation as RE ion, B cation as Fe ion, and oxygen ion, respectively. Therefore, the perovskite structure is generally considered to be a stable phase, when the tolerance factor,

$t = [(r_A + r_O)]/[\sqrt{2}(r_B + r_O)]$ is close to 1 (Schneider et al., 1961; Woodward, 1997; Li et al., 2004). Regarding the relationship between RE elements and tradition metal ions, the tolerance factor decreases with decreasing ionic radius of the RE element (Kumar et al., 2011); that is, the perovskite structure becomes less stable. However, for $REFeO_3$, the orthorhombic phase is thermodynamically stable for all RE elements, and the trend is different from a general trend observed in $REMnO_3$ (**Figure 1A**); orthorhombic $REMnO_3$ (o-$REMnO_3$) with a perovskite structure and the space group of $Pbnm$ is preferentially formed for RE elements with large ionic sizes (La–Dy), while hexagonal $REMnO_3$ (h-$REMnO_3$) with $P6_3cm$ is obtained for RE elements with small ionic sizes (Ho–Lu and Y) (**Figures 1B,C**). As the ionic size of an Fe^{3+} ion is almost the same as that of an Mn^{3+} ion, the difference in the electronic configuration of d orbitals between Fe^{3+} and Mn^{3+} ions may contribute to the stability of the hexagonal phase. In other words, because h-$REFeO_3$ is a thermodynamically unstable phase, it is relatively poorly studied compared with o-$REFeO_3$.

By controlling the synthetic route, h-$REFeO_3$ composed from RE ions with a smaller ionic radius than Er or Y have been obtained. The space group of h-$REFeO_3$ has been reported as $P6_3cm$ with a $YMnO_3$ structure type or $P6_3/mmc$ with a $YAlO_3$ structure type (Li et al., 2008; Kumar et al., 2009; Magome et al., 2010). The crystal structure belonging to $P6_3cm$ is very similar to that to $P6_3/mmc$, except for a slightly more distorted crystal structure in the former than in the latter. Actually, the oxygen layer has a zigzag structure in the $P6_3cm$ structure. In either space

group, h-$REFeO_3$ has a unique crystal structure other than the coordination state of Fe^{3+} ion; RE and Fe layers are alternately stacked along the c-axis. $REFe_2O_4$ or $RE_2Fe_3O_7$, represented by the chemical formula $RE_nFe_{n+1}O_{(3n+1)}$, are known as hexagonal phase-related materials (Malaman et al., 1976; Qin et al., 2009; Bourgeois et al., 2012; Lafuerza et al., 2014), and the coordination environment of Fe ions is a trigonal bipyramidal structure similar to the structure of h-$REFeO_3$. $REFe_2O_4$ has a hexagonal layer structure with the space group of $R\bar{3}m$, which is formed by the alternate stacking of two layers with compositions of $REO_{3/2}$ and $Fe^{2+}Fe^{3+}O_{5/2}$ (**Figure 1D**). The Fe layer consists of two triangular sheets of corner-sharing FeO_5 trigonal bipyramids. $RE_2Fe_3O_7$ can be transcribed to $REFe_2O_4\bullet(REFeO_3)$, and the structures of the $REFe_2O_4\bullet(REFeO_3)_n$ phases are described by alternately stacking $REFe_2O_4$ and hexagonal $REFeO_3$ blocks along the c-axis direction (**Figure 1E**).

When h-$REFeO_3$ is viewed as an applied material, its layered structure composed of RE and Fe layers along the c-axis is very attractive for multiple purposes, from electric to catalytic applications. In fact, $LuFe_2O_{4+x}$ has shown excellent oxygen storage properties because its hexagonal-related structure has unique structural flexibility accompanied by "topotactic transition" during the oxygen intercalation/de-intercalation process (Hervieu et al., 2014). In this transformation, the original cation ordering in the hexagonal structure is maintained without any intermixing between RE and Fe ions. This mini-review therefore presents the method for controlling the crystal structure of h-$REFeO_3$ and o-$REFeO_3$ and discusses the catalytic properties of h-$REFeO_3$.

FIGURE 1 | (A) Tolerance factor and stable crystal structure against ionic size of RE in $REMnO_3$, **(B)** Orthorhombic $REFeO_3$ (o-$REFeO_3$) or o-$REMnO_3$ with the space group of $Pbnm$, **(C)** Hexagonal $REFeO_3$ (h-$REFeO_3$) or h-$REMnO_3$ with the space group of $P6_3cm$, **(D)** $REFe_2O_4$, and **(E)** $RE_2Fe_3O_7$.

SOLVOTHERMAL METHOD

Because h-REFeO$_3$ is a metastable phase, a unique synthesis method is typically required. Among existing methods, a solvothermal method is effective for controlling the hexagonal and orthorhombic phases. In this method, synthesis of inorganic material is achieved by reaction in a liquid medium at high temperatures in a closed vessel (autoclave) (Demazeau, 1999; Cushing et al., 2004). Therefore, the traditional solvothermal method is a hydrothermal method in which water is used as the solvent. Since the last three decades, alcohol or glycol has been used as a solvent in the solvothermal method (Fanelli and Burlew, 1986; Das et al., 2008), with which various metal oxides or mixed oxides with unique morphology or ultrafine nanoparticles have been reported.

Inoue et al. found that h-REFeO$_3$ nanoparticles composed of RE with a smaller ionic radius than Er can be obtained through a non-aqueous solvothermal reaction of RE acetate with Fe acetylacetonate in 1,4-butanediol at 300°C (**Figure 2**; Inoue et al., 1997). It should be noted that crystal growth in the c-axis direction in h-REFeO$_3$ is drastically suppressed during solvothermal synthesis, resulting in the formation of nanoparticles with a particle size of approximately 20 nm and a well-formed hexagonal plate-like morphology. It was found that h-YbFeO$_3$ and o-YbFeO$_3$ can be controlled by the choice of reaction conditions and the starting material for the solvothermal reaction (Hosokawa et al., 2009). Interestingly, when RE chloride (RE = Sm-Yb) and Fe acetylacetonate are used for the solvothermal reaction in 1,4-butanediol in the presence of hexamethylenediamine, monodisperse particles of o-REFeO$_3$ (crystallite size: about 80 nm) are formed. It is suggested that o-YbFeO$_3$ has a larger crystallite size than solvothermally-synthesized h-YbFeO$_3$, which indicates that crystal nucleation is more difficult for o-YbFeO$_3$ than h-YbFeO$_3$.

High-resolution transmission electron microscopy (TEM) of Yb$_3$Fe$_4$O$_{10}$ revealed that three or more YbFeO$_3$ layers are inserted between the YbFe$_2$O$_4$ layers (Matsui et al., 1979),

suggesting that the REFe$_2$O$_4$ phase with Fe^{3+} and Fe^{2+} species may act as a nucleus for h-REFeO$_3$. The result indicates that the existence of Fe^{2+} ions plays an important role in the formation of h-REFeO$_3$. The solvothermal reaction in 1,4-butanediol causes reductive conditions because of the reducing ability of glycol; that is, Fe^{2+} species formed in the reaction system seem to contribute to the formation of h-REFeO$_3$. On the other hand, because the incorporation of amine into the solvothermal reaction suppresses the reduction from Fe^{3+} to Fe^{2+} ions owing to the chelating ability of hexamethylenediamine, o-YbFeO$_3$ must be obtained. In addition, the reducibility of Fe^{3+} species is unsurprisingly also considered to depend on whether the ligand of the starting material is acetate or chloride.

This non-aqueous solvothermal method enables the crystallization of REFeO$_3$ nanoparticles below 100 nm without calcination. Therefore, it is promising to control the crystal structure, shape, and particle size by adjusting the additives and solvent in the solvothermal system.

COPRECIPITATION AND SOL-GEL METHOD

General synthetic routes such as the coprecipitation method inevitably involve a calcination process for the synthesis of metal oxide materials, and it is difficult to synthesize the metastable phase. Therefore, h-REFeO$_3$ is often synthesized by optimizing the crystallization process. For example, h-REFeO$_3$ is synthesized by introducing solutions containing metal salts into a high-temperature inductively coupled plasma (ICP) (Mizoguchi et al., 1996). An instant crystallization under the ICP atmosphere yields h-REFeO$_3$ nanoparticles sized 20–50 nm. Kumar et al. reported that the hexagonal phase is synthesized by rapidly cooling a melt of the composition REFeO$_3$ under controlled oxygen pressure (Vijaya Kumar et al., 2008). This method requires special equipment in which the precursor is suspended on a nozzle fitted to an oxygen gas jet, thereby preventing heterogeneous
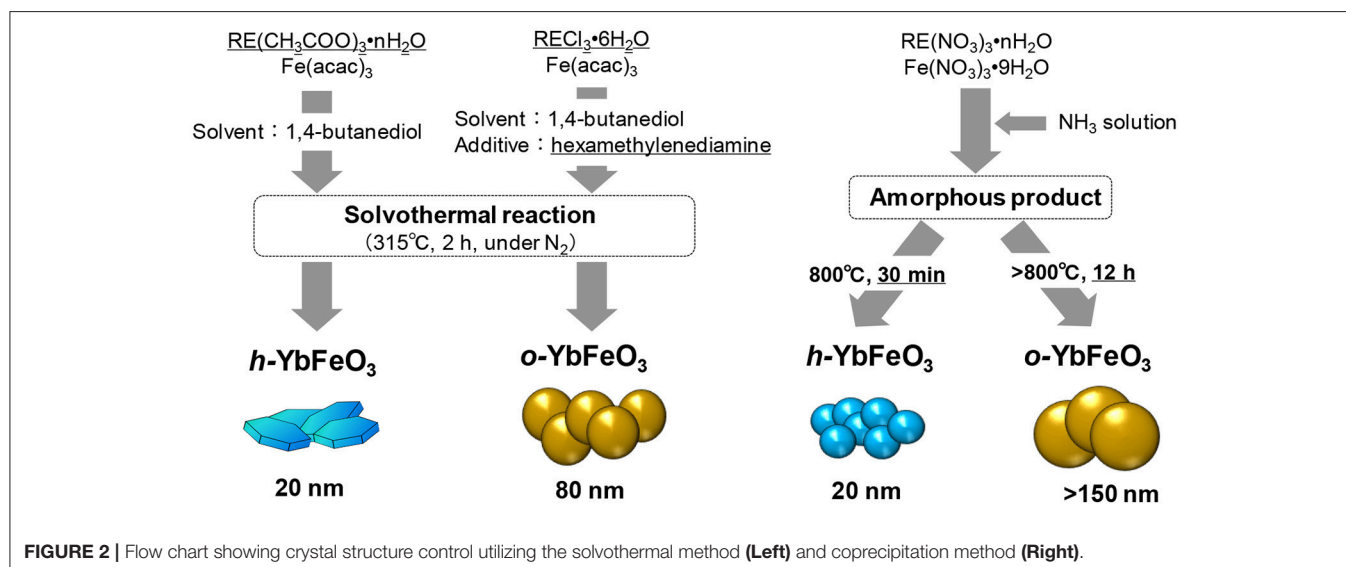

FIGURE 2 | Flow chart showing crystal structure control utilizing the solvothermal method **(Left)** and coprecipitation method **(Right)**.

nucleation that occurs on the walls of the container. As a result, h-LuFeO$_3$ with high crystallinity is obtained under an oxygen partial pressure of 1×10^5 Pa.

On the other hand, in the case of h-REFeO$_3$ synthesis from an amorphous precursor obtained by coprecipitation method in which ammonia water is added immediately to an aqueous solution containing RE and Fe ions (Nishimura et al., 2013), h-REFeO$_3$ for RE ions with a smaller ionic radius than Er can be easily obtained under precisely controlled calcination conditions. For an amorphous precursor with the composition of YbFeO$_3$, an exothermic peak without weight change is observed in the temperature range slightly below 800°C, by thermal gravimetric-differential thermal analysis. Therefore, the sample calcined in air at 700°C for 30 min is amorphous, and the formation of pure-phase h-YbFeO$_3$ is confirmed by calcining the amorphous product at 800°C for 30 min (**Figure 2**). Note that, when the retention time at 800°C is extended to 12 h, o-YbFeO$_3$ is obtained as the main product. These results strongly suggest that the exothermic peak is attributed not only to crystallization from an amorphous to hexagonal structure but also a phase transition from a hexagonal structure to orthorhombic structure. In other words, the hexagonal and orthorhombic phase can be kinetically classified by adjusting the heat retention time in the calcination process. In this manner, because a subtle change in calcination conditions leads to the formation of h-REFeO$_3$ from an amorphous product, the synthesis of h-REFeO$_3$ is much more difficult than that of o-REFeO$_3$.

Similar crystallization behavior is also observed for a precursor containing organic species synthesized by a citric acid-assisted sol-gel process (Zhang et al., 2012). For an amorphous precursor with the composition of YFeO$_3$, the crystallization temperature of h-YFeO$_3$ is 700°C. This is lower than that of h-YbFeO$_3$ (800°C); therefore, the crystallization temperature depends on the ionic radius of RE ions. Interestingly, doping Pd on h-YFeO$_3$ via the sol-gel method stabilizes the hexagonal phase, and the phase transformation to the orthorhombic phase hardly proceeds even by calcination at 1,000°C (Li et al., 2008).

h-REFeO$_3$, which is obtained by the calcination of a precursor synthesized by the solution method, often comprises fine particles with a crystallite diameter below 50 nm. On the other hand, o-REFeO$_3$, which is obtained by phase transition from h-REFeO$_3$, has a much larger particle size than h-REFeO$_3$. For example, the particle size of h-YbFeO$_3$ synthesized by the coprecipitation method is approximately 20 nm, whereas that of o-YbFeO$_3$ is above 150 nm. A nucleation and growth mechanisms has been reported to proceed in a phase transition from γ-Al$_2$O$_3$ or θ-Al$_2$O$_3$ to α-Al$_2$O$_3$ (Dynys and Halloran, 1982; Bagwell et al., 2001): that is, rapid crystal growth of α-Al$_2$O$_3$ simultaneously progresses with the formation of crystal nuclei of α-Al$_2$O$_3$, resulting in the formation of α-Al$_2$O$_3$ with a very large particle size. Similar to the phenomena for α-Al$_2$O$_3$, crystal nucleation and rapid crystal growth of o-REFeO$_3$ must proceed during the phase transition from h-REFeO$_3$ to o-REFeO$_3$. These results imply that h-REFeO$_3$ nanoparticles can be synthesized by the coprecipitation or sol-gel method, but o-REFeO$_3$ with a particle size below 100 nm is difficult to synthesize for RE ions with a smaller ionic radius than Er.

CATALYTIC PERFORMANCE OF H-REFEO$_3$

o-REFeO$_3$ has been applied as a catalyst material in various fields including the purification of volatile organic compound etc. (Ciambelli et al., 2001; Barbero et al., 2006). Applications of h-REFeO$_3$ have been rare, except for in magnetic or electronic fields, until about 15 years ago. However, recent applications have emerged in the field of catalysts (Kurzman et al., 2011; Ismael et al., 2017). For example, h-YFeO$_3$ has been reported to show a higher catalytic activity than o-YFeO$_3$ for the photodecomposition of methyl orange under visible light irradiation (> 420 nm) (Zhang et al., 2012). As h-YFeO$_3$ (1.94 eV) has a narrower band gap than o-YFeO$_3$ (2.43 eV), the band structure of h-YFeO$_3$ may be contributed to the high catalytic activity. h-YFeO$_3$ with the unique band structure is also demonstrated to be suitable as a photoanode for solar water splitting (Guo et al., 2017).

The catalytic performance of h-REFeO$_3$ as an oxidation catalyst has actively been investigated. When CH$_4$ oxidations over h-YbFeO$_3$ and o-YbFeO$_3$ obtained by the solvothermal reaction are evaluated (Hosokawa et al., 2011), the h-YbFeO$_3$ catalysts shows extremely high combustion activity compared with o-YbFeO$_3$. The T_{50} value, at which the catalyst exhibits 50% CH$_4$ conversion, is 475°C for h-YbFeO$_3$, while that for o-YbFeO$_3$ 550°C. The surface area of the o-YbFeO$_3$ catalyst significantly decreases during calcination at 800°C in catalyst preparation; that is, the surface area of o-YbFeO$_3$ synthesized by the solvothermal method is 26 m^{2}g^{-1} and that of o-YbFeO$_3$ after calcination is 6 m^{2}g^{-1}. Interestingly, the surface area of the h-YbFeO$_3$ catalyst (approximately 30 m^{2}g^{-1}) does not change significantly during the calcination, and the well-formed hexagonal plate shape is maintained. This result suggests that the surface energy of o-YbFeO$_3$ is higher than that of h-YbFeO$_3$. In other words, because h-YbFeO$_3$ synthesized by the solvothermal method has high thermal stability, high catalytic activity must be achieved.

The h-YFe$_{1-x}$Pd$_x$O$_{3-\delta}$ catalyst synthesized by the sol-gel method has been reported to show high catalytic activity ($T_{50} =$ 100°C) for CO oxidation under excess O$_2$ concentration (1,000 ppm CO and 10% O$_2$), comparable to that of a Pd/Al$_2$O$_3$ catalyst with high surface area (Li et al., 2008). The ionic Pd species in the hexagonal lattice contributes to the catalytic activity. Lu et al. also reported that a Pd catalyst supported on h-YFeO$_3$ is more effective for CH$_4$ oxidation than Pd/h-YMnO$_3$ or Pd/o-LaFeO$_3$, and that the Pd/YFeO$_3$ catalyst maintains a high catalytic activity for CH$_4$ oxidation even after aging treatment at 900°C despite the phase transformation to o-YFeO$_3$ (Lu et al., 2014a,b, 2015). In these cases, as the Pd species is adequately anchored with the h-YFeO$_3$ support, the catalyst seems to have high catalytic activity.

Furthermore, to develop a noble-metal free h-YbFeO$_3$-based catalyst with high catalytic activity, transition metal-modified h-YbFeO$_3$ catalysts are synthesized by solvothermal methods (Hosokawa et al., 2016). Mn modification by the solvothermal method dramatically improves the catalytic activity of h-YbFeO$_3$ itself for CO oxidation in which a reaction gas composed of 5,000 ppm CO and 5,000 ppm O$_2$ is introduced on catalyst bed.

The catalytic activity ($T_{50} = 120°C$) of Mn-modified h-YbFeO$_3$ (Mn-h-YbFeO$_3$) with the composition of YbFe$_{0.6}$Mn$_{0.4}$O$_3$ exceeds that ($T_{50} = 134°C$) of the noble metal Pd/Al$_2$O$_3$ catalyst.

CONCLUSION

Conventionally, a special method has been required for the synthesis of h-REFeO$_3$ due to its metastable nature; however, h-REFeO$_3$ can now be easily synthesized by precisely controlling the calcination process even when employing the coprecipitation or sol-gel methods. h-REFeO$_3$-based materials have been demonstrated to be applicable for catalyst materials, as well as magnetic or electronic materials. I believe that excellent catalyst

materials will evolve from catalyst designs focusing on the unique crystal structure of h-REFeO$_3$ or hexagonal-related materials (RE$_n$Fe$_{n+1}$O$_{(3n+1)}$).

AUTHOR CONTRIBUTIONS

The author confirms being the sole contributor of this work and has approved it for publication.

ACKNOWLEDGMENTS

REFERENCES

Bagwell, R. B., Messing, G. L., and Howell, P. R. (2001). The formation of α-Al$_2$O$_3$ from θ-Al$_2$O$_3$: the relevance of a "critical size" and: diffusional nucleation or "synchro-shear"? *J. Mater. Sci.* 36, 1833–1841. doi: 10.1023/A:1017545213590

Barbero, B. P., Gamboa, J. A., and Cadus, L. E. (2006). Synthesis and characterization of La$_{1−x}$Ca$_x$FeO$_3$ perovskite-type oxide for total oxidaiton of volatile organic compound. *Appl. Catal. B Environ.* 65, 21–30. doi: 10.1016/j.apcatb.2005.11.018

Bourgeois, J., Hevieu, M., Poienar, M., Abakumov, A. M., Elkaim, E., Sougrati, M. T., et al. (2012). Evidence of oxygen-dependent modulation in LuFe$_2$O$_4$. *Phys. Rev. B* 85:064102. doi: 10.1103/PhysRevB.85.064102

Ciambelli, P., Cimino, S., Rossi, S., Lisi, L., Minelli, G., Porta, P., et al. (2001). AFeO$_3$ (A = La, Nd, Sm) and LaFe$_{1−x}$Mg$_x$O$_3$ perovskites as methane combustion and CO oxidation catalysts: structual, redox and catalytic properties. *Appl. Catal. B Environ.* 29, 239–250. doi: 10.1016/S0926-3373(00)00215-0

Cushing, B. L., Kolesnichenko, V. L., and O'Connor, C. J. (2004). Recent advances in liquid-phase syntheses of inorganic nanoparticles. *Chem. Rev.* 104, 3893–3946. doi: 10.1021/cr030027b

Das, S., Chauduri, S., and Maji, S. (2008). Ethanol-water mediated solvothermal synthesis of cube and pyramid shaped nanostructured tin oxide. *J. Phys. Chem. C* 112, 6213–6219. doi: 10.1021/jp800612v

Demazeau, G. (1999). Solvothermal processes: a route to the stabilization of new materials. *J. Mater. Chem.* 9, 15–18. doi: 10.1039/a805536j

Dynys, F. W., and Halloran, J. W. (1982). Alpha-alumina formation in alum-derived gamma-alumina. *J. Am. Ceram. Soc.* 65, 442–448. doi: 10.1111/j.1151-2916.1982.tb10511.x

Fanelli, A. J., and Burlew, J. (1986). Preparation of fine alumina powder in alcohol. *J. Am. Ceram. Soc.* 69, C174–C175. doi: 10.1111/j.1151-2916.1986.tb04828.x

Guo, Y., Zhang, N., Huang, H., Li, Z., and Zou, Z. (2017). A novel wide-spectrum response hexagonal YFeO$_3$ photoanode for solar water splitting. *RSC Adv.* 7, 18418–18420. doi: 10.1039/C6RA28390J

Hervieu, M., Guesdon, A., Bourgeois, J., Elkaim, E., Poienar, M., Damay, F., et al. (2014). Oxygen storage capacity and structural flexibility of LuFe$_2$O$_{4+x}$ (0≤x≤0.5). *Nat. Mater.* 13, 74–80. doi: 10.1038/nmat3809

Hosokawa, S., Jeon, H.-J., and Inoue, M. (2011). Thermal stabilities of hexagonal and orthorhombic YbFeO$_3$ synthesized by solvothermal method and their catalytic activities for methane combustion. *Res. Chem. Intermed.* 37, 291–296. doi: 10.1007/s11164-011-0251-9

Hosokawa, S., Jeon, H.-J., Iwamoto, S., and Inoue, M. (2009). Synthesis of rare earth iron-mixed oxide nanoparticles by solvothermal methods. *J. Am. Ceram. Soc.* 92, 2847–2853. doi: 10.1111/j.1551-2916.2009.03295.x

Hosokawa, S., Tada, R., Shibano, T., Matsumoto, S., Teramura, K., and Tanaka, T. (2016). Promoter effect of Pd species on Mn oxide catalysts supported on rare-earth-iron mixed oxide. *Catal. Sci. Technol.* 6, 7868–7874. doi: 10.1039/C6CY01462C

Inoue, M., Nishikawa, T., Nakamura, T., and Inui, T. (1997). Glycothermal reaction of rare-earth acetate and iron acetylacetonate: formation of hexagonal REFeO$_3$. *J. Am. Ceram. Soc.* 80, 2157–2160. doi: 10.1111/j.1151-2916.1997.tb03103.x

Ismael, M., Elhaddad, E., Taffa, D., and Wark, M. (2017). Synthesis of phase pure hexagonal YFeO$_3$ perovskite as efficient visible light active photocatalyst. *Catalysts* 7:326. doi: 10.3390/catal7110326

Kumar, M. S. V., Higaki, N., Kuribayashi, K., Hibiya, T., and Yoda, S. (2011). Formation of orthorhombic and multiferroic hexagonal phases from an undercooled RMnO$_3$ (R=Rare-Earth Element) melt using a containerless technique. *J. Am. Ceram. Soc.* 94, 281–288. doi: 10.1111/j.1551-2916.2010.04042.x

Kumar, M. S. V., Kuribayashi, K., and Kitazono, K. (2009). Effect of oxygen partial pressure on the formation of metastable phases from an undercooled YbFeO$_3$ melt using an aerodynamic levitator. *J. Am. Ceram. Soc.* 92, 903–910. doi: 10.1111/j.1551-2916.2009.02974.x

Kurzman, J. A., Li, J., Schladt, T. D., Parra, C. R., Ouyang, X., Davis, R., et al. (2011). Pd^{2+}/Pd^0 redox cycling in hexagonal YMn$_{0.5}$Fe$_{0.5}$O$_3$: implications for catalysis by PGM-substituted complex oxides. *Inorg. Chem.* 50, 8073–8084. doi: 10.1021/ic200455a

Lafuerza, S., García, J., Subías, G., Blasco, J., and Cuartero, V. (2014). Strong local lattice instability in hexagonal ferrites RFe$_2$O$_4$ (R= Lu,Y,Yb) revealed by x-ray absorption spectroscopy. *Phys. Rev. B* 89:045129. doi: 10.1103/PhysRevB.89.045129

Li, C., Soh, K. C. K., and Wu, P. (2004). Formability of ABO$_3$ perovskites. *J. Alloys Compd.* 372, 40–48. doi: 10.1016/j.jallcom.2003.10.017

Li, J., Singh, U. G., Schladt, T. D., Stalick, J. K., Scott, S. L., and Seshadri, R. (2008). Hexagonal YFe$_{1−x}$Pd$_x$O$_{3−δ}$: nonperovskite host compounds for Pd^{2+} and their catalytic activity for CO oxidation. *Chem. Mater.* 20, 6567–6576. doi: 10.1021/cm801534a

Lu, Y., Keav, S., Maegli, A. E., Weidenkaff, A., and Ferri, D. (2015). Pd loading and structure of flame-made Pd/YFeO$_{3±δ}$. *Top. Catal.* 58, 910–918. doi: 10.1007/s11244-015-0459-9

Lu, Y., Keav, S., Marchionni, V., Chiarello, G. L., Pappacena, A., Di Michiel, M., et al. (2014a). Ageing induced improvement of methane oxidation activity of Pd/YFeO$_3$. *Catal. Sci. Technol.* 4, 2919–2931. doi: 10.1039/C4CY00289J

Lu, Y., Michalow, K. A., Matam, S. K., Winkler, A., Maegli, A. E., Yoon, S., et al. (2014b). Methane abatement under stoichiometric conditions on perovskite-supported palladium catalysts prepared by flame spray synthesis. *Appl. Catal. B Environ.* 144, 631–643. doi: 10.1016/j.apcatb.2013.08.001

Magome, E., Moriyoshi, C., Kuroiwa, Y., Masuno, A., and Inoue, H. (2010). Noncentrosymmetric structure of LuFeO$_3$ in metastable state. *Jpn. J. Appl. Phys.* 49:09ME06. doi: 10.1143/JJAP.49.09ME06

Malaman, B., Tanniere, N., Courtoas, A., and Protas, J. (1976). Structure cristalline de la phase Yb$_2$Fe$_3$O$_7$. *Acta Cryst. B* 32, 749–752. doi: 10.1107/S0567740876003919

Matsui, Y., Kato, K., Kimizuka, N., and Horiuchi, S. (1979). Structure image of $Yb_3Fe_4O_{10}$ by a 1 MV high-resolution electron microscope. *Acta Cryst. B* 35, 561–564. doi: 10.1107/S0567740879004155

Mizoguchi, Y., Onodera, H., Yamauchi, H., Kagawa, M., Syono, Y., and Hirai, T. (1996). Mossbauer spectra and magnetic susceptibilities of ultrafine hexagonal $RFeO_3$ (R = Eu, Yb) particles formed by the spray inductively coupled plasma technique. *Mater. Sci. Eng. A* 217/218, 164–166. doi: 10.1016/S0921-5093(96)10339-7

Nishimura, T., Hosokawa, S., Masuda, Y., Wada, K., and Inoue, M. (2013). Synthesis of metastable rare-earth–iron mixed oxide with the hexagonal crystal structure. *J. Solid State Chem.* 197, 402–407. doi: 10.1016/j.jssc.2012.08.056

Qin, Y. B., Yang, H. X., Zhang, Y., Tian, H. F., Ma, C., Zhao, Y. G., et al. (2009). The effect of Mg doping on the structural and physical properties of $LuFe_2O_4$ and $Lu_2Fe_3O_7$. *J. Phys. Condens. Matter.* 21:015401. doi: 10.1088/0953-8984/21/1/015401

Schneider, S. J., Roth, R. S., and Waring, J. L. (1961). Solid state reactions involving oxides of trivalent cations. *J. Res. Nat. Bur. Stand. A* 65, 345–374. doi: 10.6028/jres.065A.037

Vijaya Kumar, M. S., Nagashio, K., Hibiya, T., and Kuribayashi, K. (2008). Formation of hexagonal metastable phases from an undercooled $LuFeO_3$ melt in an atmosphere with low oxygen partial pressure. *J. Am. Ceram. Soc.* 91, 806–812. doi: 10.1111/j.1551-2916.2007.02200.x

Woodward, P. M. (1997). Octahedral tilting in perovskites. II. structure stabilizing forces. *Acta Cryst. B* 53, 44–46.

Zhang, Y., Yang, J., Xu, J., Gao, Q., and Hong, Z. (2012). Controllable synthesis of hexagonal and orthorhombic $YFeO_3$ and their visible-light photocatalytic activities. *Mater. Lett.* 81, 1–4. doi: 10.1016/j.matlet.2012.04.080